Analytical and Numerical Solutions for Nonlinear Equations
©Available online at https://ansne.du.ac.ir/
Online ISSN: 3060–785X
2025, Volume 10, Issue 1, pp. 100–114
Research article

Mathematical Modeling of Cancer: Sensitivity Analysis of Tumor Growth Rate and the Effect of Anti-TIGIT Treatment Dosage

Masoumeh Ahmadi[1], Afshin Babaei[1,*]

[1] Department of Applied Mathematics, University of Mazandaran, P.O. Box 47416-95447, Babolsar, Iran

*** Corresponding author(s):** babaei@umz.ac.ir

Received: 11/10/2025 **Revised:** 22/11/2025 **Accepted:** 28/11/2025 **Published:** 17/12/2025 10.22128/ansne.2025.3092.1162

Abstract

This study develops a mathematical model for cancer using a system of nonlinear differential equations to analyze tumor dynamics and the effects of Anti-TIGIT treatment. By computing the net growth rate, we evaluate the potential for tumor proliferation and establish its relationship with the stability of equilibrium points. Additionally, a sensitivity analysis is performed to identify the key parameters influencing tumor growth. These insights are then used to guide the dosage of Anti-TIGIT treatment and to inform effective therapeutic strategies by targeting the most influential and adjustable factors.

Keywords: Immunotherapy, Mathematical model, Net growth rate, Sensitivity analysis, Anti-TIGIT.

Mathematics Subject Classification (2020): 92B05, 49K40, 65L15

1 Introduction

Immune checkpoint inhibitors, a form of immunotherapy targeting specific membrane proteins on T cells and cancer cells, have revolutionized cancer treatment, improving patient outcomes through innovative therapeutic approaches. Despite significant advancements, drug resistance remains a significant challenge, hindering the effectiveness of these therapies [34, 38]. By harnessing the body's natural immune system to identify and eliminate cancer cells, immunotherapy offers the potential for more precise and effective treatments with fewer side effects.

Within the field of cancer immunotherapy, the role of immune co-inhibitory receptors has garnered significant attention [39]. These receptors, which include ITIM-bearing receptors such as TIGIT, play crucial roles in regulating immune responses and maintaining immune homeostasis. However, their overexpression or dysregulation in the tumor microenvironment can enable cancer cells to evade immune detection, contributing to tumor growth and progression [30, 32].

TIGIT (also known as WUCAM, VSTM3, or Vsig9) is an inhibitory molecule expressed on $CD4^+$ and $CD8^+$ T lymphocytes and NK lymphocytes [9, 41]. It consists of an extracellular immunoglobulin variable (IgV) domain, a type 1 transmembrane domain and a cytoplasmic tail with an immunoreceptor tyrosine-based inhibitory motif (ITIM) and an Ig tail-tyrosine (ITT)-like motif [19].

The immunosuppressive action of TIGIT is caused by several mechanisms. TIGIT can inhibit $CD8^+$ T lymphocyte proliferation by acting directly on the formation of the TCR complex [19]. Also, TIGIT inhibits NK cells directly and blunt their production of interferon

gamma [25].

While all co-inhibitory receptors can suppress T-cell activation, they differ in potency, kinetics of expression, and the specific cellular signaling pathways they modulate. Whereas the co-inhibitory checkpoint CTLA-4 acts downstream of TCR-induced signaling by targeting downstream effectors of PI3K through activation of the serine/threonine phosphatase PP2A, TIGIT operates more upstream. TIGIT inhibits $CD8^+$ T-cell proliferation and activation by directly affecting TCR expression, as engagement of TIGIT induces down-regulation of the TCR-α chain and other components of the TCR complex In addition, TIGIT reduces TCR-induced p-ERK signaling in $CD8^+$ T cells. Binding of TIGIT on NK cells to its ligand CD155 suppresses NK-cellmediated cytotoxicity and IFN-γ production through signaling cascades elicited by ITIM and ITT-like motifs in its cytoplasmic tail. However, TIGIT exerts its functions not only through direct cell-intrinsic inhibitory signaling but also indirectly. Similar to CTLA-4, which blocks the binding of its co-stimulatory counterpart CD28 to their shared ligands CD80 and CD86, TIGIT can compete with CD226 for ligand binding, thereby reducing CD226-mediated T-cell co-stimulation. TIGIT can also inhibit co-stimulatory signaling by preventing CD226 homodimerization. Moreover, TIGIT suppresses T-cell responses indirectly by modulating the functions of cells expressing its ligand CD155. TIGIT expressed on $CD4^+$ T cells induces IL-10 and suppresses IL-12 production by dendritic cells via CD155 engagement, thereby inhibiting $CD4^+$ T-cell proliferation and IFN-γ production [19].

Statistical analyses of clinical studies have shown that TIGIT can be detected in different stages of melanoma, which is closely related to the occurrence, development, and prognosis of melanoma. This review mainly describes the immunosuppressive mechanism of TIGIT and its role in antitumor immunity of melanoma, aiming to offer new insights and therapeutic strategies for TIGIT-targeted treatment of melanoma [9, 35].

At low tumor-cell densities, tumor growth can deviate from classical exponential models and instead exhibit cooperative behavior consistent with an Allee effect, in which the net growth rate increases with cell number [22]. In this setting, the sign of the net growth rate r determines whether the tumor population expands or declines: if $r > 0$, each cell effectively contributes to producing more than one new cell on average, allowing the tumor population to grow. Conversely, if $r < 0$, the number of cells decreases over time, leading to eventual extinction of the tumor population below the Allee threshold [5]. This bistable structure highlights the importance of identifying density thresholds and parameter regimes that determine tumor persistence or elimination [22].

Many real-world biological processes can be effectively described through mathematical models [4, 15, 18]. Mathematical modeling plays a crucial role in cancer research by integrating diverse biological parameters into computational frameworks. Such models enable researchers to analyze tumor progression, predict treatment outcomes, and provide more effective treatment strategies [13, 40].

In the field of cancer immunotherapy, mathematical modeling provides several advantages [17, 28]. It enables the exploration of various treatment scenarios, the prediction of treatment outcomes, and the identification of effective dosing regimens and combination therapies. By simulating the effects of TIGIT inhibitors, researchers can evaluate the impact of these immunotherapeutic agents on the immune response, tumor growth, and overall clinical outcomes. Moreover,studies have shown that TIGIT is significantly overexpressed on tumor-infiltrating T cells. These findings suggest that the increased expression of TIGIT may be associated with T cell exhaustion [9].

In numerous research studies, sensitivity analysis is conducted to evaluate the influence of model parameters on system behavior. By systematically varying key parameters, researchers can determine their relative impact on tumor progression and treatment efficacy [11, 27]. Sensitivity analysis is usually conducted by modifying each parameter by a small value at a particular point in time [12, 14, 20]. This process allows for the determination of the output's sensitivity to each parameter, thereby identifying their relative effectiveness. Alternatively, a normalized sensitivity coefficient can be calculated to provide a dimensionless value for these sensitivity coefficients [11, 26, 27].

This study formulates a nonlinear differential equation model to analyze tumor dynamics under Anti-TIGIT treatment. By computing the net growth rate , we assess tumor proliferation potential, while sensitivity analysis identifies key parameters influencing cancer progression. Furthermore, we investigate the relationship between the net growth rate of tumor cells and equilibrium stability, offering insights into more effective treatments. Ultimately, our findings contribute to determining an appropriate dosage for Anti-TIGIT therapy, enhancing its clinical applicability.

2 Mathematical Model

The immune system comprises a diverse array of components, such as natural killer cells, dendritic cells, T cell subsets, containing $CD4^+$ T and $CD8^+$ T cells and interleukins such as IL-2 and IL-12 that play a crucial function in orchestrating immune responses. To

maintain homeostasis, the immune inhibitory molecule TIGIT serves as a critical checkpoint, suppressing excessive immune activation by down-regulating signalling pathways in immune cells. This checkpoint interacts with specific anti-ligands to fine-tune immune activity [1]. The biomathematical framework for anti-TIGIT therapies is grounded in the cancer-immune cycle, as illustrated in Figure 1 [30].

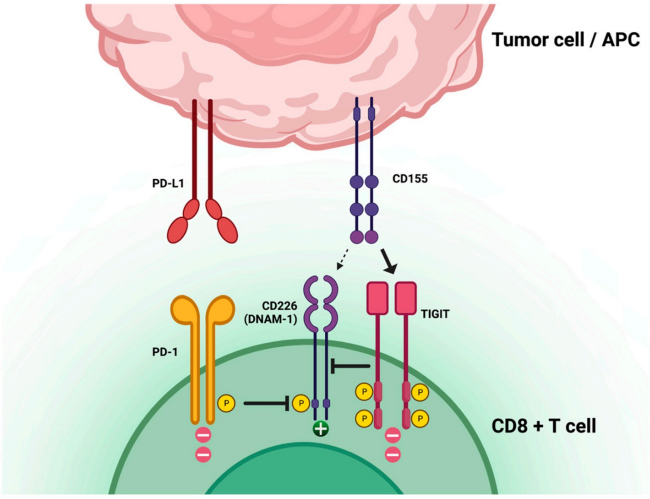

Figure 1. T-cell immunoreceptor with immunoglobulin and immunoreceptor tyrosine-based inhibitory motif domains (TIGIT) position, role, and connection to other immune-checkpoint axes. Designed with https://www.biorender.com accessed on 28 March 2023.

Figure 2. Red rectangles represent tumor cells, blue rectangles indicate immune system cells, yellow ellipses correspond to immune checkpoints, and green ellipses denote the proposed therapeutic interventions. Arrows with a pointed tip signify proliferation/activation, obstructed arrows symbolize the process of killing/blocking, and dashed lines represent the expression of proteins on T cells and NK cells. For a detailed explanation of the biological significance of each pathway, see the text in Section 2 and Figure 1.

These interactions are illustrated in Figure 2. As shown in the diagram, the resulting model comprises a system of nonlinear ordinary differential equation to describe the interactions between natural killer cells (N), T-cells (T), cytokines (I_2 and I_{12}), cancer cells (C), dendritic cells (D), the inhibitory TIGIT (G) and Anti-TIGIT (A_G). Based on these cellular relationships, the mathematical model is formulated as follows:

$$\frac{dN(t)}{dt} = s_1 + \lambda_{NI_2}N(t)\left(\frac{I_2(t)}{K_{I_2}+I_2(t)}\right)\left(\frac{1}{1+G(t)/K_G}\right) - d_N N(t), \tag{1}$$

$$\frac{dC(t)}{dt} = \lambda_C C(t)\left(1-\frac{C(t)}{S_M}\right) - (\eta_T T(t)+\eta_N N(t))C(t) - d_C C(t), \tag{2}$$

$$\frac{dD(t)}{dt} = \lambda_{DC} D_0\left(\frac{C(t)}{K_C+C(t)}\right) - d_D D(t), \tag{3}$$

$$\frac{dI_{12}(t)}{dt} = \lambda_{I_{12}D}D(t) - d_{I_{12}}I_{12}(t) \tag{4}$$

$$\frac{dT(t)}{dt} = \left[\lambda_{TI_{12}}T_0\left(\frac{I_{12}(t)}{K_{I_{12}}+I_{12}(t)}\right)+\lambda_{TI_2}T(t)\left(\frac{I_2(t)}{K_{I_2}+I_2(t)}\right)\right]\left(\frac{1}{1+G(t)/K_G}\right) - d_{I_2T}T(t)I_2(t) - d_T T(t), \tag{5}$$

$$\frac{dI_2(t)}{dt} = \lambda_{I_2T}T(t) - (d_{I_2N}N(t)+d_{I_2T}T(t))I_2(t) - d_{I_2}I_2(t), \tag{6}$$

$$\frac{dG(t)}{dt} = \frac{G(t)}{N(t)+T(t)}\left[\lambda_{NI_2}N(t)\left(\frac{I_2(t)}{K_{I_2}+I_2(t)}\right)+\lambda_{TI_{12}}T_0\left(\frac{I_{12}(t)}{K_{I_{12}}+I_{12}(t)}\right)+\lambda_{TI_2}T(t)\left(\frac{I_2(t)}{K_{I_2}+I_2(t)}\right)\right]\left(\frac{1}{1+G(t)/K_G}\right) - \frac{G(t)}{N(t)+T(t)}(d_N N(t)+d_T T(t)) - \mu_{GA_G}G(t)A_G(t), \tag{7}$$

$$\frac{dA_G(t)}{dt} = u - \mu_{GA_G} G(t) A_G(t) - d_{A_G} A_G(t). \tag{8}$$

In Eq. (1), the term $\left(\frac{I_2(t)}{K_{I_2}+I_2(t)}\right)\left(\frac{1}{1+G(t)/K_G}\right)$ represents the rate of N production stimulated by I_2 that is not inhibited by TIGIT [10, 24, 31]. In Eq. (3), $\frac{C(t)}{K_C+C(t)}$ stands for the Michaelis-Menten coefficient, which means that the activation of D is proportional to this expression. In Eq. (4), IL-12 (I_{12}) is secreted by stimulated dendritic cells (D) [21, 36]. In Eq. (5), naive T cells are activated by IL-12 (I_{12}), and IL-2 (I_2) [36]. It is assumed to be inhibited by TIGIT [3, 6, 16], which reduces the production of T cells by the factor $\frac{1}{1+\frac{G(t)}{K_G}}$. In Eq. (6), IL-2 ($I_2$) is secreted by activated T cells [21, 36]. In Eq. (7), TIGIT, which is expressed on T cells and NK cells, suppresses their activity by binding to ligands on dendritic cells or tumor cells, creating an immune checkpoint. Additionally, IL-12 from dendritic cells enhances the function of NK cells so that they can kill tumor cells directly.

A summary of the definitions and descriptions of the other parameters used in the model is provided in Table 1.

3 Model Analysis

3.1 Equilibrium Points of the Model

Equilibrium points are obtained by solving the homogeneous form of the system (1)-(8):

$$(\dot{N}, \dot{C}, \dot{D}, \dot{I_{12}}, \dot{T}, \dot{I_2}, \dot{G}, \dot{A_G})^T = 0. \tag{9}$$

Tumor-Free Equilibrium $\mathscr{E}_0$

This equilibrium occurs when the tumor is completely eliminated, i.e., $C(t) = 0$. Then:

$$\mathscr{E}_0 : \; N(t) = \frac{s_1}{d_N}, \; D(t) = 0, I_{12}(t) = 0, \; T(t) = 0, \; I_2(t) = 0, \; G(t) = 0, \; A_G = \frac{u}{d_{AG}}.$$

Endemic Equilibrium $\mathscr{E}^*$

In this state, all variables are expressed in terms of N^* and T^*:

$$\frac{\lambda_{I_2 T} T^*}{K_{I_2} A(T^*, N^*) + \lambda_{I_2 T} T^*} = \frac{d_N N^* - s_1}{\lambda_{N I_2} N^*} \left(1 + \frac{u(N^* + T^*)}{K_G\left(-s_1 + \frac{d_{I_2 T} \lambda_{I_2 T} (T^*)^2}{A(T^*, N^*)}\right)}\right),$$

$$C^* = \frac{S_M}{\lambda_C}(\lambda_C - \eta_T T^* - \eta_N N^* - d_C), \tag{10}$$

$$D^* = \frac{\lambda_{DC} D_0}{d_D}\left(\frac{C^*}{K_C + C^*}\right), \tag{11}$$

$$I_{12}^* = \frac{\lambda_{I_{12D}}}{d_{I_{12}}} D^*, \tag{12}$$

$$I_2^* = \frac{\lambda_{I_2 T} T^*}{d_{I_2 N} N^* + d_{I_2 T} T^* + d_{I_2}}, \tag{13}$$

$$G^* = \frac{u\left(N^* + T^*\right)}{\left(-s_1 + d_{I_2 T} T^* I_2^*\right)} - \frac{d_{A_G}}{\mu_{GA_G}}, \tag{14}$$

$$A_G^* = \frac{d_{I_2 T} T^* I_2^* - s_1}{\mu_{GA_G}\left(N^* + T^*\right)}. \tag{15}$$

Eq. (7) concludes that

$$\frac{dG(t)}{dt} = \frac{G(t)}{N(t) + T(t)}\left[\lambda_{N I_2} N(t) \frac{I_2(t)}{K_{I_2} + I_2(t)} + \lambda_{T I_{12}} T_0 \frac{I_{12}(t)}{K_{I_{12}} + I_{12}(t)}\right.$$

$$+\ \lambda_{TI_2}T(t)\frac{I_2(t)}{K_{I_2}+I_2(t)}\Bigg]\left(\frac{1}{1+\dfrac{G(t)}{K_G}}\right)-\frac{G(t)}{N(t)+T(t)}\big(d_N N(t)+d_T T(t)\big)-\mu_{GA_G}G(t)A_G(t)=0. \tag{16}$$

From Eq. (1):

$$\lambda_{NI_2}N(t)\left(\frac{I_2(t)}{K_{I_2}+I_2(t)}\right)\left(\frac{1}{1+\frac{G(t)}{K_G}}\right)=d_N N(t)-s_1,$$

and Eq. (5) results:

$$\left[\lambda_{TI_{12}}T_0\left(\frac{I_{12}(t)}{K_{I_{12}}+I_{12}(t)}\right)+\lambda_{TI_2}T(t)\left(\frac{I_2(t)}{K_{I_2}+I_2(t)}\right)\right]\left(\frac{1}{1+\frac{G(t)}{K_G}}\right)=d_{I_2T}T(t)I_2(t)+d_T T(t).$$

By substituting these results into equation (7), we get

$$\frac{G(t)}{N(t)+T(t)}[-s_1+d_{I_2T}T(t)I_2(t)]-\mu_{GA_G}G(t)A_G(t)=0.$$

This leads to two possibilities:

$$\begin{cases} G(t)=0, \\ A_G(t)=\dfrac{d_{I_2T}T(t)I_2(t)-s_1}{\mu_{GA_G}\big(N(t)+T(t)\big)}. \end{cases} \tag{17}$$

If $G(t)=0$, then the homogeneous form of Eq. (8) yields

$$A_G(t)=\frac{u}{d_{A_G}}.$$

If $G(t)\neq 0$, then the homogeneous forms of Eq. (8) and Eq. (17) yield

$$G(t)=\frac{u\mu_{GA_G}\big(N(t)+T(t)\big)}{\mu_{GA_G}(-s_1+d_{I_2T}T(t)I_2(t))}-\frac{d_{A_G}}{\mu_{GA_G}}. \tag{18}$$

From Eqs. (2), (3) and (4) we have:

$$C(t)=\frac{s_M}{\lambda_C}\left(\lambda_C-\eta_T T(t)+\eta_N N(t)+d_C\right), \tag{19}$$

$$D(t)=\frac{\lambda_{DC}D_0}{d_D}\left(\frac{C(t)}{K_C+C(t)}\right), \tag{20}$$

$$I_{12}(t)=\frac{\lambda_{I_{12}D}}{d_{I_{12}}}D(t). \tag{21}$$

From Eq. (6):

$$I_2(t)=\frac{\lambda_{I_2T}T(t)}{d_{I_2N}N(t)+d_{I_2T}T(t)+d_{I_2}}. \tag{22}$$

Also, using Eq. (18) and the homogeneous form of Eq. (1):

$$\frac{I_2(t)}{K_{I_2}+I_2(t)}=\frac{d_N N(t)-s_1}{\lambda_{NI_2}N(t)}\left(1+\frac{\frac{u\mu_{GA_G}\left(N(t)+T(t)\right)}{\mu_{GA_G}\left(-s_1+d_{I_2T}T(t)I_2(t)\right)}-\frac{d_{A_G}}{\mu_{GA_G}}}{K_G}\right). \tag{23}$$

From the equality of Eq. (22) and Eq. (23), $N^*(t)$ and $T^*(t)$ are also obtained from the following equation:

$$\frac{\lambda_{I_2T}T(t)}{K_{I_2}A(T,N)+\lambda_{I_2T}T(t)}=\frac{d_N N(t)-s_1}{\lambda_{NI_2}N(t)}\left(1+\frac{u(N(t)+T(t))}{K_G\left(-s_1+\dfrac{d_{I_2T}\lambda_{I_2T}T(t)^2}{A(T,N)}\right)}\right),$$

where, $A(T,N)=d_{I_2N}N(t)+d_{I_2T}T(t)+d_{I_2}$.

3.2 Stability of the Tumor-Free Equilibrium

To assess local stability of the tumor-free equilibrium $\mathscr{E}_0$, we compute the net growth rate at low tumor density r using the next-generation matrix method [37].

Lemma 1. *If $\mathscr{E}_0$ is the tumor-free equilibrium, then the net growth rate at low tumor density is:*

$$r = (\mathscr{R}_{\mathscr{E}_0} - 1)(d_C + \frac{\eta_N s_1}{d_N}), \tag{24}$$

where

$$\mathscr{R}_{\mathscr{E}_0} = \frac{\lambda_C d_N}{\eta_N s_1 + d_C d_N}. \tag{25}$$

Moreover,

$$\mathscr{R}_{\mathscr{E}_0} > 1 \iff r > 0, \qquad \mathscr{R}_{\mathscr{E}_0} < 1 \iff r < 0.$$

Proof. Consider the system (1)-(8). The matrices $\mathscr{F}$ and $\mathscr{V}$ are defined as follows:

$$\mathscr{F} = \begin{bmatrix} \lambda_C C(t) \\ 0 \end{bmatrix}, \quad \mathscr{V} = \begin{bmatrix} \lambda_C C(t) \frac{C(t)}{S_M} + (\eta_T T(t) + \eta_N N(t)) C(t) + d_C C(t) \\ d_D D(t) - \lambda_{DC} D_0 \left(\frac{C(t)}{K_C + C(t)} \right) \end{bmatrix}.$$

Therefore,

$$D\mathscr{F} = \begin{bmatrix} F & 0 \\ 0 & 0 \end{bmatrix}, \quad D\mathscr{V} = \begin{bmatrix} V & 0 \\ -\lambda_{DC} D_0 \left(\frac{K_C}{(K_C + C(t))^2} \right) & d_D \end{bmatrix},$$

where, $F = \lambda_C$ and $V = \frac{2\lambda_C}{S_M} C(t) + \eta_T T(t) + \eta_N N(t) + d_C$. The next generation matrix defined as:

$$FV^{-1} = \frac{\lambda_C}{\frac{2\lambda_C}{S_M} C(t) + \eta_T T(t) + \eta_N N(t) + d_C}.$$

So,

$$r = (\mathscr{R}_{\mathscr{E}_0} - 1)(d_C + \frac{\eta_N s_1}{d_N}), \tag{26}$$

is the net growth rate at low tumor density in $\mathscr{E}_0$, where $\mathscr{R}_{\mathscr{E}_0} = \frac{\lambda_C d_N}{\eta_N s_1 + d_C d_N}$.

Also, it is clear from Eqs. (24) and (25) that

$$\mathscr{R}_{\mathscr{E}_0} > 1 \iff r > 0, \qquad \mathscr{R}_{\mathscr{E}_0} < 1 \iff r < 0.$$

□

Theorem 1. *The equilibrium point $\mathscr{E}_0$ is locally asymptotically stable if $r < 0$, and unstable if $r > 0$.*

Proof. The entries of the Jacobian matrix for the cancer model are as follows:

$$j_{11} = \lambda_{NI_2} \left(\frac{I_2}{k_{I_2} + I_2} \right) \left(\frac{1}{1 + \frac{G}{k_G}} \right) - d_N, \qquad j_{16} = \lambda_{NI_2} N \left(\frac{k_{I_2}}{(k_{I_2} + I_2)^2} \right) \left(\frac{1}{1 + \frac{G}{k_G}} \right),$$

$$j_{17} = -\frac{\lambda_{NI_2} N I_2}{k_G (k_{I_2} + I_2) \left(1 + \frac{G}{k_G}\right)^2}, \qquad j_{21} = -\eta_N C,$$

$$j_{22} = \lambda_C \left(1 - \frac{2C}{s_m}\right) - (\eta_T T + \eta_N N) - d_C, \qquad j_{25} = -\eta_T C,$$

$$j_{32} = \lambda_{DC} D_0 \left(\frac{k_C}{(k_C + C)^2} \right), \qquad j_{33} = -d_D,$$

$$j_{43} = \lambda_{I_{12} D}, \qquad j_{44} = -d_{I_{12}},$$

$$j_{54} = \lambda_{TI_{12}} T_0 \left(\frac{k_{I_{12}}}{(k_{I_{12}} + I_{12})^2}\right)\left(\frac{1}{1+\frac{G}{k_G}}\right), \qquad j_{61} = -d_{I_2N} I_2,$$

$$j_{65} = \lambda_{I_2T} - d_{I_2T} I_2, \qquad j_{66} = -d_{I_2N} N - d_{I_2T} T - d_{I_2},$$

$$j_{74} = \frac{G}{N+T}\frac{\lambda_{TI_{12}} T_0}{k_{I_{12}} + I_{12}}\frac{1}{1+\frac{G}{k_G}}, \qquad j_{78} = -\mu_{GA_G} G,$$

$$j_{87} = -\mu_{GA_G} A_G, \qquad j_{88} = -\mu_{GA_G} G - d_{A_G},$$

$$j_{55} = \lambda_{TI_2}\left(\frac{I_2}{k_{I_2}+I_2}\right)\left(\frac{1}{1+\frac{G}{k_G}}\right) - d_{I_2T} I_2 - d_T,$$

$$j_{56} = \lambda_{TI_2} T\left(\frac{k_{I_2}}{(k_{I_2}+I_2)^2}\right)\left(\frac{1}{1+\frac{G}{k_G}}\right) - d_{I_2T} T,$$

$$j_{57} = -\frac{1}{k_G\left(1+\frac{G}{k_G}\right)^2}\left(\lambda_{TI_{12}}\frac{I_{12}}{k_{I_{12}}+I_{12}} + \lambda_{TI_2} T\frac{I_2}{k_{I_2}+I_2}\right),$$

$$j_{75} = \left(\frac{G}{N+T}\right)\left(\lambda_{NI_2} N\frac{I_2}{k_{I_2}+I_2} + \lambda_{TI_{12}} T_0\frac{I_{12}}{k_{I_{12}}+I_{12}} + \lambda_{TI_2} T\frac{I_2}{k_{I_2}+I_2}\right)\left(\frac{1}{1+\frac{G}{k_G}}\right)$$
$$- \frac{G}{(N+T)^2} d_T - \mu_{GA_G} G A_G,$$

$$j_{76} = \frac{G}{N+T}\left(\lambda_{NI_2} N\frac{1}{k_{I_2}+I_2} - \lambda_{NI_2} N\frac{I_2}{(k_{I_2}+I_2)^2} + \lambda_{TI_2} T\frac{1}{k_{I_2}+I_2} - \lambda_{TI_2} T\frac{I_2}{(k_{I_2}+I_2)^2}\right)\left(\frac{1}{1+\frac{G}{k_G}}\right)$$
$$- \frac{G}{(N+T)^2}(d_N N + d_T T) - \mu_{GA_G} G A_G,$$

$$j_{77} = \frac{1}{N+T}\left(\lambda_{NI_2} N\frac{I_2}{k_{I_2}+I_2} + \lambda_{TI_{12}} T_0\frac{I_{12}}{k_{I_{12}}+I_{12}} + \lambda_{TI_2} T\frac{I_2}{k_{I_2}+I_2}\right)\left(-\frac{1}{k_G}\frac{G}{\left(1+\frac{G}{k_G}\right)^2}\right)$$
$$- \frac{1}{N+T}(d_N N + d_T T) - \mu_{GA_G} A_G,$$

The remaining entries are zero.

As a result, the entries of Jacobian matrix at the tumor-free equilibrium point, $\mathscr{E}_0$, are in the following form:

$$j_{11} = -d_N, \quad j_{16} = \frac{\lambda_{NI_2} s_1}{d_N k_{I_2}}, \quad j_{17} = 0, \quad j_{21} = 0,$$

$$j_{22} = \lambda_C - \frac{\eta_N s_1}{d_N} - d_C, \quad j_{25} = 0, \quad j_{32} = \frac{\lambda_{DC} D_0}{k_C}, \quad j_{33} = -d_D,$$

$$j_{43} = \lambda_{I_{12}D}, \quad j_{44} = -d_{I_{12}}, \quad j_{54} = \frac{\lambda_{TI_{12}} T_0}{k_{I_{12}}}, \quad j_{55} = -d_T,$$

$$j_{56} = 0, \quad j_{57} = 0, \quad j_{61} = 0, \quad j_{65} = \lambda_{I_2T},$$

$$j_{66} = -d_{I_2N}\frac{s_1}{d_N} - d_{I_2}, \quad j_{74} = 0, \quad j_{75} = 0, \quad j_{76} = 0,$$

$$j_{77} = -\frac{d_N N + d_T T}{N+T} - \mu_{GA_G} A_G, \quad j_{78} = 0,$$

$$j_{87} = -\mu_{GA_G}\frac{u}{d_{AG}}, \quad j_{88} = -d_{A_G},$$

Then, the eigenvalues of $J(\mathscr{E}_0)$ are as:

$$\lambda_1 = -d_N, \quad \lambda_2 = \lambda_C - \eta_N\frac{s_1}{d_N} - d_C, \quad \lambda_3 = -d_D,$$

$$\lambda_4 = -d_{I_{12}}, \quad \lambda_5 = -d_T, \quad \lambda_6 = -\frac{d_{I_2N} s_1}{d_N} - d_{I_2},$$

$$\lambda_7 = -\frac{\mu_{GA_G} u}{d_{AG}}, \qquad \lambda_8 = -d_{A_G}$$

To ensure the local asymptotic stability of $\mathscr{E}_0$, all eigenvalues must have negative real parts. All but one eigenvalue, $\lambda_2 = \lambda_C - \eta_N \frac{s_1}{d_N} - d_C$, are clearly negative. Thus, the stability of $\mathscr{E}_0$ hinges on the sign of λ_2. If $\lambda_C - \eta_N \frac{s_1}{d_N} - d_C < 0$, then $\mathscr{E}_0$ is stable; if $\lambda_C - \eta_N \frac{s_1}{d_N} - d_C > 0$, it is unstable. According to Eq. (24), the tumor-free equilibrium $\mathscr{E}_0$ is locally asymptotically stable when $r < 0$, and unstable when $r > 0$. □

4 Determining the Effective Dosage for Anti-TIGIT Therapy

In this section, we will numerically solve the model using the Adams-Bashforth method [2], and analyze the results obtained from the sensitivity analysis. The parameters and initial values used in the model are presented in Table 1. The definitions and values of the model parameters used in the numerical simulations are given below. All parameters are expressed in units of g/cm^3.

Table 1. Description of variables used in the model.

Parameter	Description	Value	References
λ_C	Proliferation rate of cancer cells	0.203	[34]
S_M	Transporting capacity of cancer cells	4.9	[34]
η_T	Killing rate of tumor cells by $CD4^+$ and $CD8^+$ T cells	33	[34]
η_N	Fractional (non)-ligand-transduced tumor cell kill by NK cells	30	Assumed
d_C	Mortality rate of tumor cells	0.17	[23]
λ_{DC}	Rate of DCs activated by cancer cell	5.2	[34]
d_D	Mortality rate of DCs	0.13	[34]
$\lambda_{I_{12}D}$	Production rate of I12 by D	3.03×10^{-6}	[34]
$d_{I_{12}}$	Degradation rate of IL-12	2.13	[34]
$K_{I_{12}}$	Half-saturation of IL-12	10^{-10}	[23]
$\lambda_{TI_{12}}$	Activation rate of $CD4^+$ and $CD8^+$ T cells by IL-12	2.75	[34]
$\lambda_{I_{12}T}$	Activation rate of IL-12 cells by $CD4^+$ and $CD8^+$ T	10^{-7}	[34]
T_0	Source of T_4 and T_8	6×10^{-4}	[34]
D_0	Source of D	2×10^{-5}	[34]
λ_{TI_2}	Activation rate of $CD4^+$ and $CD8^+$ T cells by IL-2	0.5	[23]
K_{I_2}	Half-saturation of IL-2	1.9×10^{-11}	[23]
d_{I_2T}	Production rate of IL-2 by $CD4^+$ and $CD8^+$ T cells	2.7	Assumed
λ_{I_2T}	Decay of I12 due to T4	1.6×10^{-6}	[34]
d_T	Death rate of $CD4^+$ and $CD8^+$ T cells	0.377	[23]
d_{I_2N}	Production rate of NK cells by IL-2	1.02×10^{-2}	[11]
d_{I_2}	Degradation rate of IL-2	166.22	[34]
K_G	Rate of inhibition	1.8×10^{-2}	Assumed
K_C	Half saturation of D	4×10^{-4}	[34]
λ_{NI_2}	Maximum production rate of NK cells due to the influence of IL-2	6.68×10^{-3}	[29]
s_1	Constant influx rate of the NK cells	1.32×10^{-4}	Assumed
d_N	Death rate NK cells	9.8×10^{-2}	[29]
μ_{GA_G}	Rate of depletion of A_G by G	5.8×10^4	fitted
d_{A_G}	Anti-TIGIT degraded rate	0.02	Assumed

We simulated the model (1)–(8) using the initial conditions expressed in units of g/cm^3, where $N(0) = 4.4 \times 10^{-2}$, $C(0) = 0.41$, $D(0) = 6 \times 10^{-4}$, $I_{12}(0) = 1.8 \times 10^{-10}$, $T(0) = 6 \times 10^{-3}$, $I_2(0) = 1.5 \times 10^{-11}$, $G(0) = 11.2 \times 10^{-10}$, $A_G(0) = 0$.

4.1 Sensitivity Analysis of the Net Growth Rate for Dosage Determination

Sensitivity indices are useful for evaluating how changes in model parameters influence state variables. The normalized forward sensitivity index is defined as the ratio of the relative change in a variable to the relative change in a parameter. If the variable is a differentiable function of the parameter, this index can also be expressed in terms of partial derivatives.

Given the explicit formula for $\mathscr{R}_{\mathscr{E}_0}$ in Eq. (25), we can infer an analytical expression for the sensitivity index, denoted by $S_p = \frac{\partial \mathscr{R}_{\mathscr{E}_0}}{\partial p} \cdot \frac{p}{\mathscr{R}_{\mathscr{E}_0}}$, as referenced in [8]. This index is computed for each of the five key parameters as follows:

$$S_{\lambda_C} = 1, \qquad S_{\eta_N} = -\frac{\eta_N \cdot \frac{s_1}{d_N}}{\eta_N \cdot \frac{s_1}{d_N} + d_C}, \qquad S_{s_1} = -\frac{\eta_N \cdot \frac{s_1}{d_N}}{\eta_N \cdot \frac{s_1}{d_N} + d_C},$$

$$S_{d_N} = \frac{\eta_N \cdot \frac{s_1}{d_N}}{\eta_N \cdot \frac{s_1}{d_N} + d_C}, \qquad S_{d_C} = -\frac{d_C}{\eta_N \cdot \frac{s_1}{d_N} + d_C}.$$

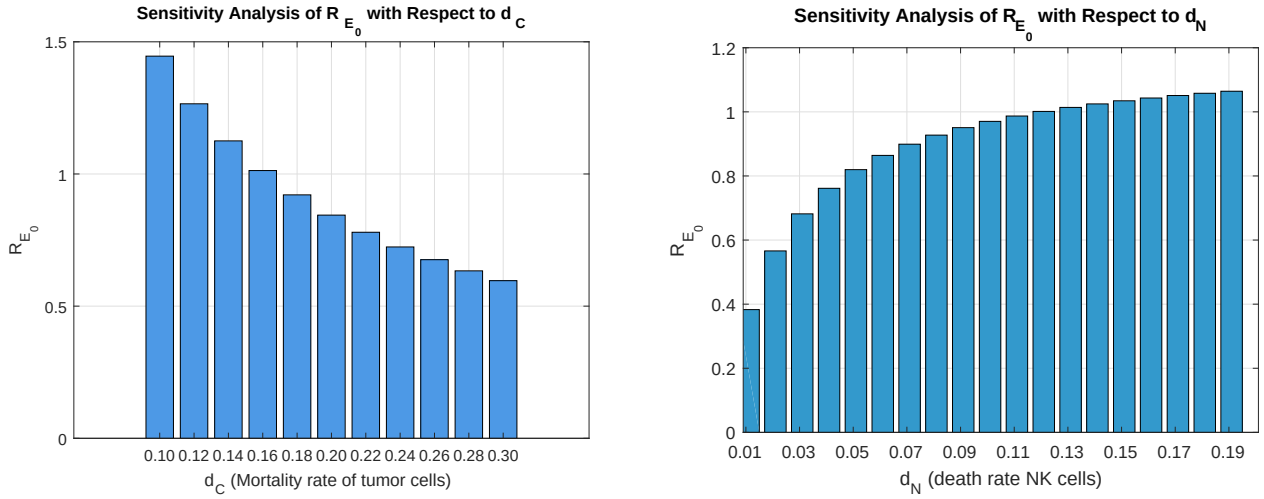

Figure 3. Sensitivity Analysis of R_{E_0} concerning d_C and d_N.

Figure 4. Sensitivity Analysis of R_{E_0} concerning η_N and s_1.

The sensitivity analysis of $\mathscr{R}_{\mathscr{E}_0}$ is shown in Figures 3, 4 and 5. These plots illustrate the degree of dependence of each parameter affecting $\mathscr{R}_{\mathscr{E}_0}$, and they also identify the ranges of the parameter within which the tumor level changes.

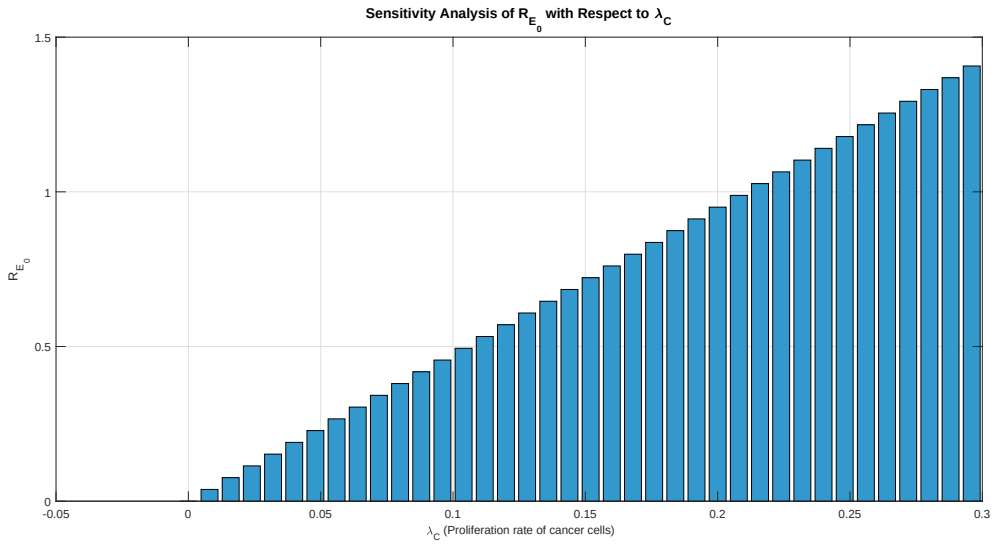

Figure 5. Sensitivity Analysis of $\mathscr{R}_{\mathscr{E}_0}$ concerning λ_C.

4.2 Treatment Strategy Informed by Sensitivity Analysis

In this subsection, we perform a sensitivity analysis of the parameters that influence the net growth rate of tumor cells and the stability of the tumor-free equilibrium point.

Figure 6 shows the extent of tumor surface change in the absence of drug, in a state where the rate of cancer cell production increases, and also in a state where the rate of cancer cell production changes in the presence of drug. One of the parameters that influences the growth and proliferation of cancer cells is λ_C. Based on the sensitivity analysis presented, this parameter has a direct influence on the net growth rate of tumor cells and consequently on tumor progression. From this analysis, when $\lambda_C < 0.203$, we have $\mathscr{R}_{\mathscr{E}_0} < 1$, indicating that treatment is not necessary. For $\lambda_C > 0.203$, the effects of treatment are illustrated in Figure 6.

Figure 7 shows the effect of the rate of cancer cell destruction by natural killer cells (η_N) compared to the effect of the drug in reducing tumor level. Additionally, the parameter η_N has an inverse effect on the net growth rate of tumor cells. Based on the corresponding sensitivity analysis, if $\eta_N < 30$, then the net growth rate of tumor cells satisfies $r > 0$, or equivalently $\mathscr{R}_{\mathscr{E}_0} > 1$, which leads to tumor progression. Therefore, treatment is necessary in such cases.

Other parameters, such as d_C, d_N, and s_1, in the net growth rate cannot be changed by treatment. These parameters are inherent to the natural system of the body and the biological cycle of cancer.

In Figure 8, the effect of of two drug dosages on the system was investigated. As can be observed, the variation of drug dosage has a significant impact on the results. This indicates that the dosage of the drug is a critical and decisive factor for the effectiveness of the treatment. In other words, the choice of an appropriate drug dosage can directly affect the treatment outcome, which emphasizes the importance of accurate dosage adjustment in the treatment protocols.

In Figure 9, the simultaneous effect of two parameters, λ_C and η_N, was investigated. Figure 9 (left) shows the effect of two factors on the expansion or reduction of tumor burden in the absence of a drug. An increase in the cancer cell production rate (λ_C) combined with a decrease in their destruction rate by natural killer cells (η_N) leads to an increase in tumor level, whereas decreasing λ_C together with increasing η_N result in a reduction of tumor level. Figure 9 (right) shows the effect of the drug in reducing tumor level, even in cases where the tumor production rate is high and the destruction rate of tumor cells by natural killer cells is low.

The sensitivity analysis helps determine the extent to which each parameter must be modified in order to reduce $\mathscr{R}_{\mathscr{E}_0}$ below 1. We can use this information to prescribe the appropriate medication and its dosage. Mathematical models and their analysis therefore play an important role in medicine, as they help in the treatment of diseases and even determine the effective therapeutic approach.

The bifurcation diagram presented in Figure 10 shows the dynamic behavior of the system across a range of values for the drug dose parameter u. (For details on the bifurcation, see [7]). As shown, the steady-state tumor cell population varies significantly with different

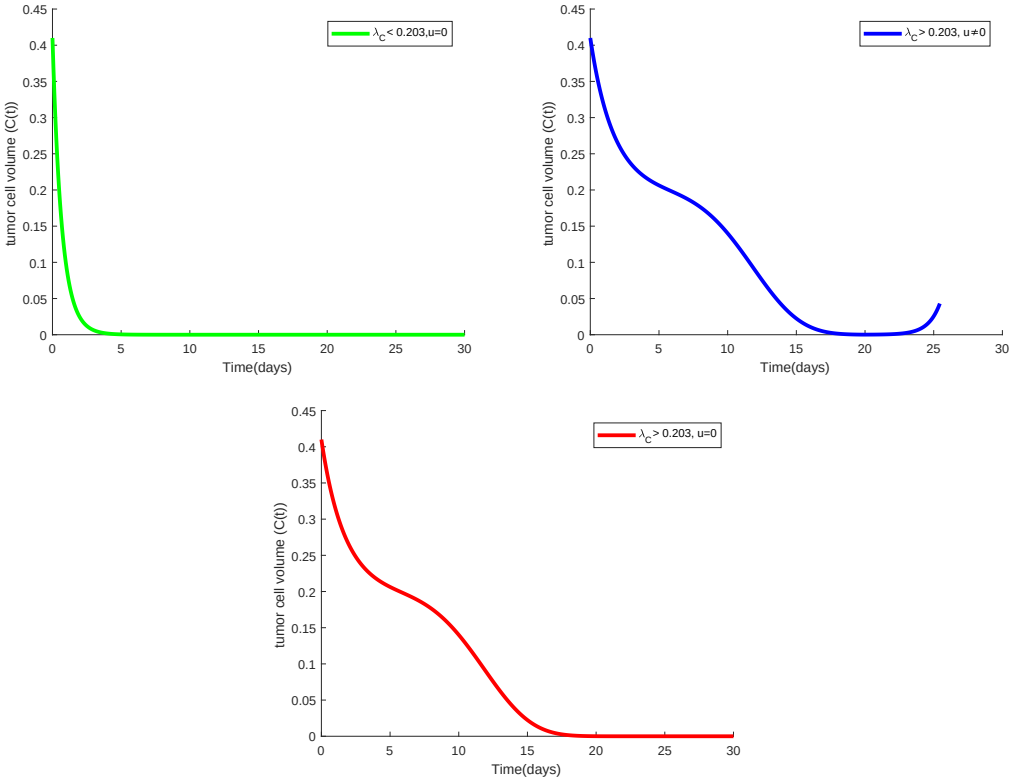

Figure 6. Impact of λ_C and Anti-TIGIT.

doses of the drug.

5 Conclusion

This study introduces a detailed mathematical cancer model formulated as a system of nonlinear differential equations to investigate the dynamics of tumor growth and treatment strategies. By calculating the net growth rate, valuable insights into the potential of tumor proliferation and the efficacy of the Anti-TIGIT drug are obtained. The stability analysis performed within the model highlights critical equilibrium points and provides a deeper understanding of the conditions required to control or eliminate tumor growth. In addition, sensitivity analysis highlights the importance of various parameters that influence the net tumor growth and helps identify key factors that impact treatment efficacy. This research ultimately contributes to optimizing Anti-TIGIT dosing, thereby facilitating the development of more effective cancer therapies and improving patient outcomes.

Authors' Contributions

All authors have the same contribution.

Data Availability

The manuscript has no associated data or the data will not be deposited.

Conflicts of Interest

The authors declare that there is no conflict of interest.

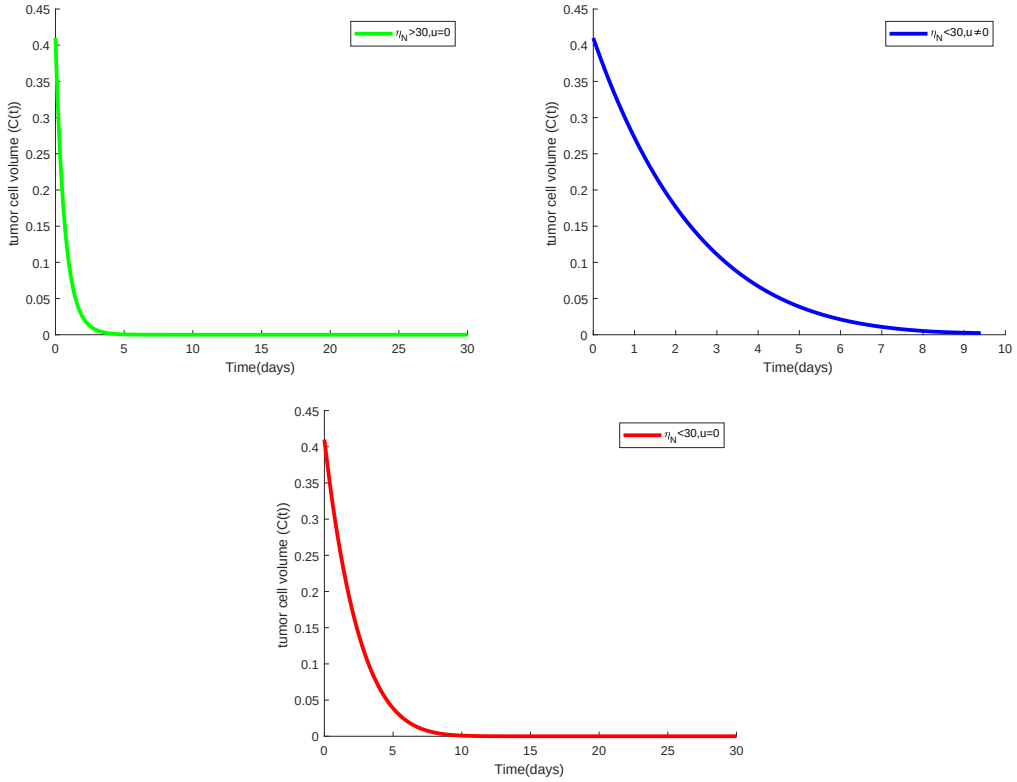

Figure 7. Impact of η_N and Anti-TIGIT.

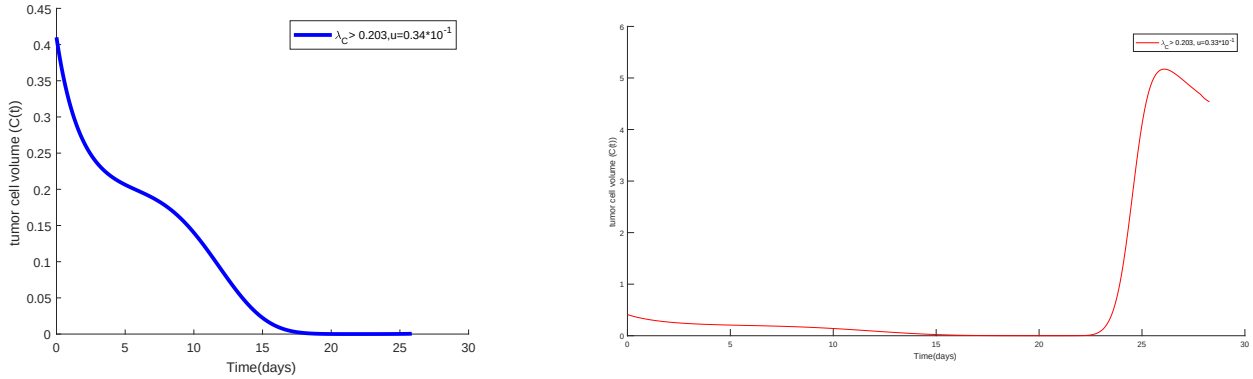

Figure 8. The impact of various drug dosages.

Ethical Considerations

The authors have diligently addressed ethical concerns, such as informed consent, plagiarism, data fabrication, misconduct, falsification, double publication, redundancy, submission, and other related matters.

Funding

This research did not receive any grant from funding agencies in the public, commercial, or nonprofit sectors.

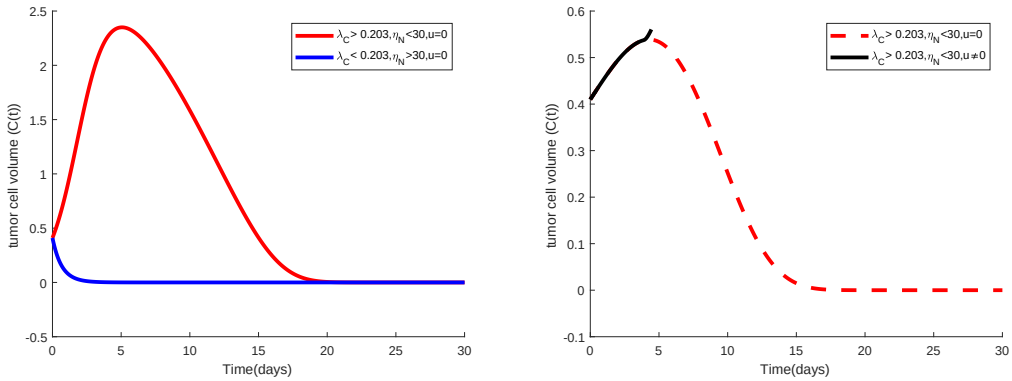

Figure 9. Impact of λ_C and η_N.

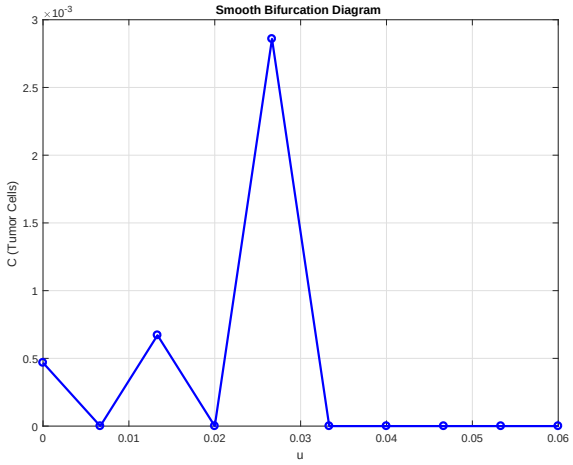

Figure 10. Bifurcation diagrams of the tumor cell model (1)-(8) for $u \in [0, 0.06]$.

Acknowledgments

The authors thank the editor and reviewers for their helpful comments.

References

[1] H. Alemohammad, B. Najafzadeh, Z. Asadzadeh, A. Baghbanzadeh, F. Ghorbaninezhad, A. Najafzadeh, H. Safarpour, R. Bernardini, O. Brunetti, M. Sonnessa, et al., The importance of immune checkpoints in immune monitoring: a future paradigm shift in the treatment of cancer, Biomedicine & Pharmacotherapy, 146, 112516, (2022).

[2] A. Babaei, H. Jafari, M. Ahmadi, A fractional order HIV/AIDS model based on the effect of screening of unaware infectives, Mathematical Methods in the Applied Sciences, 42(7), 2334–2343, (2019).

[3] L. Bergantini, M. Spalletti, M. d'Alessandro, M. Genovese, E. Masotto, P. Cameli, A. Prasse, E. Bargagli, Predictive role of natural killer cells in bronchoalveolar lavage fluid of patients with sarcoidosis, Pulmonology, 31(1), 2416867, (2024).

[4] R. Boroghani, and K. Nouri, Solving the Fractional HIV Model using Bell Polynomials and the Tau Method, Analytical and Numerical Solutions for Nonlinear Equations, 9(1), 65-73 (2025).

[5] K. Böttger, H. Hatzikirou, A. Voss-Böhme, E. A. Cavalcanti-Adam, M. A. Herrero, A. Deutsch, An emerging Allee effect is critical for tumor initiation and persistence, PLOS Computational Biology, 11(9), e1004366, (2015).

[6] J. A. Bridge, J. C. Lee, A. Daud, J. W. Wells, J. A. Bluestone, Cytokines, chemokines, and other biomarkers of response for checkpoint inhibitor therapy in skin cancer, Frontiers in Medicine, 5, 351, (2018).

[7] N. Chitnis, J. M. Cushing, J. Hyman, Bifurcation analysis of a mathematical model for malaria transmission, SIAM Journal on Applied Mathematics, 67(1), 24–45, (2006).

[8] N. Chitnis, J. M. Hyman, J. M. Cushing, Determining important parameters in the spread of malaria through the sensitivity analysis of a mathematical model, Bulletin of Mathematical Biology, 70, 1272–1296, (2008).

[9] H. Cui, M. Hamad, E. Elkord, TIGIT in cancer: from mechanism of action to promising immunotherapeutic strategies, Cell Death & Disease, 16(1), 664, (2025).

[10] M. d'Alessandro, E. Conticini, L. Bergantini, F. Mezzasalma, P. Cameli, S. Baglioni, M. Armati, M. Abbritti, E. Bargagli, PD-1, CTLA-4 and TIGIT expression on T and NK cells in granulomatous diseases: sarcoidosis and ANCA-associated vasculitis, International Journal of Molecular Sciences, 24(1), 256, (2022).

[11] L. G. de Pillis, W. Gu, A. E. Radunskaya, Mixed immunotherapy and chemotherapy of tumors: modeling, applications and biological interpretations, Journal of Theoretical Biology, 238(4), 841–862, (2006).

[12] L. G. de Pillis, A. E. Radunskaya, Modeling tumorimmune dynamics, Mathematical Models of Tumor-Immune System Dynamics, Springer New York, 59–108, (2014).

[13] R. Eftimie, J. L. Bramson, D. J. Earn, Interactions between the immune system and cancer: a brief review of non-spatial mathematical models, Bulletin of Mathematical Biology, 73(2), 2–32, (2011).

[14] H. A. Elkaranshawy, A. M. Makhlouf, Parameter estimation and sensitivity analysis for a model of tumorimmune interaction in the presence of immunotherapy and chemotherapy, Journal of the Egyptian Mathematical Society, 30(1), 8, (2022).

[15] S. Foadian, A.S. Ghadami, Z. Khalili, and H. Badamchi Zadeh, Applications of the Natural-Adomian Decomposition Method to Estimate the Parameters of HIV Infection Model of $CD4^+$ T-Cells. Analytical and Numerical Solutions for Nonlinear Equations, 6(2), 293-301 (2021).

[16] G. J. Freeman, A. J. Long, Y. Iwai, K. Bourque, T. Chernova, H. Nishimura, L. J. Fitz, N. Malenkovich, T. Okazaki, M. C. Byrne, et al., Engagement of the PD-1 immunoinhibitory receptor by a novel B7 family member leads to negative regulation of lymphocyte activation, The Journal of Experimental Medicine, 192(7), 1027–1034, (2000).

[17] S. S. Gaikwad, A. L. Zanje, J. D. Somwanshi, Advancements in transdermal drug delivery: a comprehensive review of physical penetration enhancement techniques, International Journal of Pharmaceutics, 652, 123856, (2024).

[18] A. Gambo, M. Jiya, A. K. Dotia, and K. J. Augustina, Deterministic Model of Corruption Dynamics in Nigeria VIA Homotopy Perturbation Method, Analytical and Numerical Solutions for Nonlinear Equations, 8(1), 35-52(2024).

[19] Z. Ge, M. P. Peppelenbosch, D. Sprengers, J. Kwekkeboom, TIGIT: the next step toward successful combination immune checkpoint therapy in cancer, Frontiers in Immunology, 12, 699895, (2021).

[20] R. Gul, C. Schütte, S. Bernhard, Mathematical modeling and sensitivity analysis of arterial anastomosis in the arm, Applied Mathematical Modelling, 40(17-18), 7724–7738, (2016).

[21] Y. Ma, G. V. Shurin, Z. Peiyuan, M. R. Shurin, Dendritic cells in the cancer microenvironment, Journal of Cancer, 4, 36–44, (2013).

[22] K. E. Johnson, G. Howard, W. Mo, M. K. Strasser, E. A. Lima, S. Huang, A. Brock, Cancer cell population growth kinetics at low densities deviate from the exponential growth model and suggest an Allee effect, PLOS Biology, 17(8), e3000399, (2019).

[23] X. Lai, A. Friedman, Combination therapy of cancer with cancer vaccine and immune checkpoint inhibitors: a mathematical model, PLOS One, 12(5), e0178479, (2017).

[24] B. R. Lauwerys, N. Garot, J.-C. Renauld, F. A. Houssiau, Cytokine production and killer activity of NK/T-NK cells derived with IL-2, IL-15 or the combination of IL-12 and IL-18, The Journal of Immunology, 165(4), 1847–1853, (2000).

[25] M. Li, P. Xia, Y. Du, S. Liu, G. Huang, J. Chen, H. Zhang, N. Hou, X. Cheng, L. Zhou, P. Li, X. Yang, Z. Fan, T-cell immunoglobulin and ITIM domain (TIGIT) receptor/poliovirus receptor (PVR) ligand engagement suppresses interferon-γ production of natural killer cells via β-arrestin-2-mediated negative signaling, Journal of Biological Chemistry, 289(25), 17647–17657, (2014).

[26] A. M. Makhlouf, H. A. Elkaranshawy, Sensitivity analysis for a mathematical model of tumorimmune interactions, UPB Scientific Bulletin, Series A, 83(2), 317–326, (2021).

[27] A. Makhlouf, L. El-Shennawy, H. Elkaranshawy, Mathematical modelling for the role of $CD4^+$ T cells in tumorimmune interactions, Computational and Mathematical Methods in Medicine, 2020, 7187602, (2020).

[28] K. Monica, J. Shreeharsha, P. Falkowski-Gilski, Melanoma skin cancer detection using Mask-RCNN with modified GRU model, Frontiers in Physiology, 14, 1324042, (2024).

[29] R. Padmanabhan, N. Meskin, A.-E. Al Moustafa, Mathematical Models of Cancer and Different Therapies, Springer, Singapore, (2021).

[30] J. Rivera, A. Digklia, A. S. Christou, J. Anibal, K. A. Vallis, B. J. Wood, E. Stride, A review of ultrasound-mediated checkpoint inhibitor immunotherapy, Ultrasound in Medicine & Biology, 50(1), 1-7, (2024).

[31] A. Rousseau, C. Parisi, F. Barlesi, Anti-TIGIT therapies for solid tumors: a systematic review, ESMO Open, 8(2), 101184, (2023).

[32] S. Rui, X. Kong, J. Liu, L. Wang, X. Wang, X. Zou, X. Zheng, F. Ye, H. Xu, Z. Li, et al., The landscape of TIGIT target and clinical application in diseases, MedCommOncology, 1(2), e18, (2022).

[33] S. S. Salim, J. Malinzi, E. Mureithi, N. Shaban, Mathematical modelling of chemovirotherapy cancer treatment, International Journal of Modelling and Simulation, 45(1), 364–385, (2025).

[34] N. Siewe, A. Friedman, Optimal timing of steroid initiation in response to CTLA-4 antibody in metastatic cancer: a mathematical model, PLOS One, 17(11), e0277248, (2022).

[35] T. Tang, W. Wang, L. Gan, J. Bai, D. Tan, Y. Jiang, P. Zheng, W. Zhang, Y. He, Q. Zuo, et al., TIGIT expression in extrahepatic cholangiocarcinoma and its impact on $CD8^+$ T-cell exhaustion: implications for immunotherapy, Cell Death & Disease, 16(1), 90, (2025).

[36] J. M. Tran Janco, P. Lamichhane, L. Karyampudi, K. L. Knutson, Tumor-infiltrating dendritic cells in cancer pathogenesis, The Journal of Immunology 194 (7), 2985–2991, (2015).

[37] P. Van den Driessche, J. Watmough, Reproduction numbers and sub-threshold endemic equilibria for compartmental models of disease transmission, Mathematical Biosciences, 180(1-2), 29–48, (2002).

[38] T. Vongsavath, R. Rahmani, K. M. Tun, V. Manne, The use of fecal microbiota transplant in overcoming and modulating resistance to anti-PD-1 therapy in patients with skin cancer, Cancers, 16(3), 499, (2024).

[39] T. Wang, X. Wu, C. Guo, K. Zhang, J. Xu, Z. Li, S. Jiang, Development of inhibitors of the programmed cell death-1/programmed cell death-ligand 1 signaling pathway, Journal of Medicinal Chemistry, 62(4), 1715–1730, (2018).

[40] S. Wang, J. Lei, X. Zou, S. Jin, Integrating multiscale mathematical modeling and multidimensional data reveals the effects of epigenetic instability on acquired drug resistance in cancer, PLOS Computational Biology, 21(2), e1012815, (2025).

[41] P. Zhang, X. Liu, Z. Gu, Z. Jiang, S. Zhao, Y. Song, J. Yu, Targeting TIGIT for cancer immunotherapy: recent advances and future directions, Biomarker Research, 12(1), 7, (2024).